

Proceedings of the 12<sup>th</sup> International Conference on  
Computational Fluid Dynamics in the Oil & Gas,  
Metallurgical and Process Industries

# Progress in Applied CFD – CFD2017



SINTEF Proceedings

Editors:

Jan Erik Olsen and Stein Tore Johansen

## **Progress in Applied CFD – CFD2017**

Proceedings of the 12<sup>th</sup> International Conference on Computational Fluid Dynamics  
in the Oil & Gas, Metallurgical and Process Industries

SINTEF Academic Press

SINTEF Proceedings no 2

Editors: Jan Erik Olsen and Stein Tore Johansen

**Progress in Applied CFD – CFD2017**

Selected papers from 10<sup>th</sup> International Conference on Computational Fluid Dynamics in the Oil & Gas, Metallurgical and Process Industries

Key words:

CFD, Flow, Modelling

Cover, illustration: Arun Kamath

ISSN 2387-4295 (online)

ISBN 978-82-536-1544-8 (pdf)

© Copyright SINTEF Academic Press 2017

The material in this publication is covered by the provisions of the Norwegian Copyright Act. Without any special agreement with SINTEF Academic Press, any copying and making available of the material is only allowed to the extent that this is permitted by law or allowed through an agreement with Kopinor, the Reproduction Rights Organisation for Norway. Any use contrary to legislation or an agreement may lead to a liability for damages and confiscation, and may be punished by fines or imprisonment

SINTEF Academic Press

Address:       Forskningsveien 3 B  
                  PO Box 124 Blindern  
                  N-0314 OSLO

Tel:             +47 73 59 30 00

Fax:            +47 22 96 55 08

[www.sintef.no/byggforsk](http://www.sintef.no/byggforsk)

[www.sintefbok.no](http://www.sintefbok.no)

**SINTEF Proceedings**

SINTEF Proceedings is a serial publication for peer-reviewed conference proceedings on a variety of scientific topics.

The processes of peer-reviewing of papers published in SINTEF Proceedings are administered by the conference organizers and proceedings editors. Detailed procedures will vary according to custom and practice in each scientific community.

## PREFACE

This book contains all manuscripts approved by the reviewers and the organizing committee of the 12th International Conference on Computational Fluid Dynamics in the Oil & Gas, Metallurgical and Process Industries. The conference was hosted by SINTEF in Trondheim in May/June 2017 and is also known as CFD2017 for short. The conference series was initiated by CSIRO and Phil Schwarz in 1997. So far the conference has been alternating between CSIRO in Melbourne and SINTEF in Trondheim. The conferences focuses on the application of CFD in the oil and gas industries, metal production, mineral processing, power generation, chemicals and other process industries. In addition pragmatic modelling concepts and bio-mechanical applications have become an important part of the conference. The papers in this book demonstrate the current progress in applied CFD.

The conference papers undergo a review process involving two experts. Only papers accepted by the reviewers are included in the proceedings. 108 contributions were presented at the conference together with six keynote presentations. A majority of these contributions are presented by their manuscript in this collection (a few were granted to present without an accompanying manuscript).

The organizing committee would like to thank everyone who has helped with review of manuscripts, all those who helped to promote the conference and all authors who have submitted scientific contributions. We are also grateful for the support from the conference sponsors: ANSYS, SFI Metal Production and NanoSim.

Stein Tore Johansen & Jan Erik Olsen



Organizing committee:

Conference chairman: Prof. Stein Tore Johansen

Conference coordinator: Dr. Jan Erik Olsen

Dr. Bernhard Müller

Dr. Sigrid Karstad Dahl

Dr. Shahriar Amini

Dr. Ernst Meese

Dr. Josip Zoric

Dr. Jannike Solsvik

Dr. Peter Witt

Scientific committee:

Stein Tore Johansen, SINTEF/NTNU

Bernhard Müller, NTNU

Phil Schwarz, CSIRO

Akio Tomiyama, Kobe University

Hans Kuipers, Eindhoven University of Technology

Jinghai Li, Chinese Academy of Science

Markus Braun, Ansys

Simon Lo, CD-adapco

Patrick Segers, Universiteit Gent

Jiyuan Tu, RMIT

Jos Derksen, University of Aberdeen

Dmitry Eskin, Schlumberger-Doll Research

Pär Jönsson, KTH

Stefan Pirker, Johannes Kepler University

Josip Zoric, SINTEF

## CONTENTS

<b>PRAGMATIC MODELLING .....</b>	<b>9</b>
On pragmatism in industrial modeling. Part III: Application to operational drilling .....	11
CFD modeling of dynamic emulsion stability .....	23
Modelling of interaction between turbines and terrain wakes using pragmatic approach .....	29
<b>FLUIDIZED BED .....</b>	<b>37</b>
Simulation of chemical looping combustion process in a double looping fluidized bed reactor with cu-based oxygen carriers.....	39
Extremely fast simulations of heat transfer in fluidized beds.....	47
Mass transfer phenomena in fluidized beds with horizontally immersed membranes .....	53
A Two-Fluid model study of hydrogen production via water gas shift in fluidized bed membrane reactors .....	63
Effect of lift force on dense gas-fluidized beds of non-spherical particles .....	71
Experimental and numerical investigation of a bubbling dense gas-solid fluidized bed .....	81
Direct numerical simulation of the effective drag in gas-liquid-solid systems .....	89
A Lagrangian-Eulerian hybrid model for the simulation of direct reduction of iron ore in fluidized beds.....	97
High temperature fluidization - influence of inter-particle forces on fluidization behavior .....	107
Verification of filtered two fluid models for reactive gas-solid flows .....	115
<b>BIOMECHANICS.....</b>	<b>123</b>
A computational framework involving CFD and data mining tools for analyzing disease in carotid artery .....	125
Investigating the numerical parameter space for a stenosed patient-specific internal carotid artery model.....	133
Velocity profiles in a 2D model of the left ventricular outflow tract, pathological case study using PIV and CFD modeling.....	139
Oscillatory flow and mass transport in a coronary artery.....	147
Patient specific numerical simulation of flow in the human upper airways for assessing the effect of nasal surgery.....	153
CFD simulations of turbulent flow in the human upper airways .....	163
<b>OIL &amp; GAS APPLICATIONS .....</b>	<b>169</b>
Estimation of flow rates and parameters in two-phase stratified and slug flow by an ensemble Kalman filter .....	171
Direct numerical simulation of proppant transport in a narrow channel for hydraulic fracturing application .....	179
Multiphase direct numerical simulations (DNS) of oil-water flows through homogeneous porous rocks .....	185
CFD erosion modelling of blind tees .....	191
Shape factors inclusion in a one-dimensional, transient two-fluid model for stratified and slug flow simulations in pipes .....	201
Gas-liquid two-phase flow behavior in terrain-inclined pipelines for wet natural gas transportation .....	207

<b>NUMERICS, METHODS &amp; CODE DEVELOPMENT .....</b>	<b>213</b>
Innovative computing for industrially-relevant multiphase flows .....	215
Development of GPU parallel multiphase flow solver for turbulent slurry flows in cyclone.....	223
Immersed boundary method for the compressible Navier–Stokes equations using high order summation-by-parts difference operators .....	233
Direct numerical simulation of coupled heat and mass transfer in fluid-solid systems .....	243
A simulation concept for generic simulation of multi-material flow, using staggered Cartesian grids.....	253
A cartesian cut-cell method, based on formal volume averaging of mass, momentum equations.....	265
SOFT: a framework for semantic interoperability of scientific software .....	273
 <b>POPULATION BALANCE .....</b>	 <b>279</b>
Combined multifluid-population balance method for polydisperse multiphase flows .....	281
A multifluid-PBE model for a slurry bubble column with bubble size dependent velocity, weight fractions and temperature.....	285
CFD simulation of the droplet size distribution of liquid-liquid emulsions in stirred tank reactors .....	295
Towards a CFD model for boiling flows: validation of QMOM predictions with TOPFLOW experiments .....	301
Numerical simulations of turbulent liquid-liquid dispersions with quadrature-based moment methods.....	309
Simulation of dispersion of immiscible fluids in a turbulent couette flow .....	317
Simulation of gas-liquid flows in separators - a Lagrangian approach.....	325
CFD modelling to predict mass transfer in pulsed sieve plate extraction columns .....	335
 <b>BREAKUP &amp; COALESCENCE .....</b>	 <b>343</b>
Experimental and numerical study on single droplet breakage in turbulent flow .....	345
Improved collision modelling for liquid metal droplets in a copper slag cleaning process .....	355
Modelling of bubble dynamics in slag during its hot stage engineering.....	365
Controlled coalescence with local front reconstruction method .....	373
 <b>BUBBLY FLOWS .....</b>	 <b>381</b>
Modelling of fluid dynamics, mass transfer and chemical reaction in bubbly flows .....	383
Stochastic DSMC model for large scale dense bubbly flows.....	391
On the surfacing mechanism of bubble plumes from subsea gas release.....	399
Bubble generated turbulence in two fluid simulation of bubbly flow .....	405
 <b>HEAT TRANSFER .....</b>	 <b>413</b>
CFD-simulation of boiling in a heated pipe including flow pattern transitions using a multi-field concept .....	415
The pear-shaped fate of an ice melting front .....	423
Flow dynamics studies for flexible operation of continuous casters (flow flex cc).....	431
An Euler-Euler model for gas-liquid flows in a coil wound heat exchanger.....	441
 <b>NON-NEWTONIAN FLOWS.....</b>	 <b>449</b>
Viscoelastic flow simulations in disordered porous media .....	451
Tire rubber extrudate swell simulation and verification with experiments .....	459
Front-tracking simulations of bubbles rising in non-Newtonian fluids.....	469
A 2D sediment bed morphodynamics model for turbulent, non-Newtonian, particle-loaded flows.....	479

<b>METALLURGICAL APPLICATIONS.....</b>	<b>491</b>
Experimental modelling of metallurgical processes .....	493
State of the art: macroscopic modelling approaches for the description of multiphysics phenomena within the electroslag remelting process .....	499
LES-VOF simulation of turbulent interfacial flow in the continuous casting mold .....	507
CFD-DEM modelling of blast furnace tapping .....	515
Multiphase flow modelling of furnace tapholes .....	521
Numerical predictions of the shape and size of the raceway zone in a blast furnace.....	531
Modelling and measurements in the aluminium industry - Where are the obstacles? .....	541
Modelling of chemical reactions in metallurgical processes.....	549
Using CFD analysis to optimise top submerged lance furnace geometries .....	555
Numerical analysis of the temperature distribution in a martensic stainless steel strip during hardening.....	565
Validation of a rapid slag viscosity measurement by CFD.....	575
Solidification modeling with user defined function in ANSYS Fluent.....	583
Cleaning of polycyclic aromatic hydrocarbons (PAH) obtained from ferroalloys plant.....	587
Granular flow described by fictitious fluids: a suitable methodology for process simulations .....	593
A multiscale numerical approach of the dripping slag in the coke bed zone of a pilot scale Si-Mn furnace.....	599
<b>INDUSTRIAL APPLICATIONS .....</b>	<b>605</b>
Use of CFD as a design tool for a phosphoric acid plant cooling pond .....	607
Numerical evaluation of co-firing solid recovered fuel with petroleum coke in a cement rotary kiln: Influence of fuel moisture .....	613
Experimental and CFD investigation of fractal distributor on a novel plate and frame ion-exchanger .....	621
<b>COMBUSTION .....</b>	<b>631</b>
CFD modeling of a commercial-size circle-draft biomass gasifier.....	633
Numerical study of coal particle gasification up to Reynolds numbers of 1000.....	641
Modelling combustion of pulverized coal and alternative carbon materials in the blast furnace raceway .....	647
Combustion chamber scaling for energy recovery from furnace process gas: waste to value .....	657
<b>PACKED BED.....</b>	<b>665</b>
Comparison of particle-resolved direct numerical simulation and 1D modelling of catalytic reactions in a packed bed .....	667
Numerical investigation of particle types influence on packed bed adsorber behaviour .....	675
CFD based study of dense medium drum separation processes .....	683
A multi-domain 1D particle-reactor model for packed bed reactor applications.....	689
<b>SPECIES TRANSPORT &amp; INTERFACES .....</b>	<b>699</b>
Modelling and numerical simulation of surface active species transport - reaction in welding processes .....	701
Multiscale approach to fully resolved boundary layers using adaptive grids.....	709
Implementation, demonstration and validation of a user-defined wall function for direct precipitation fouling in Ansys Fluent.....	717



<b>FREE SURFACE FLOW &amp; WAVES .....</b>	<b>727</b>
Unresolved CFD-DEM in environmental engineering: submarine slope stability and other applications.....	729
Influence of the upstream cylinder and wave breaking point on the breaking wave forces on the downstream cylinder .....	735
Recent developments for the computation of the necessary submergence of pump intakes with free surfaces .....	743
Parallel multiphase flow software for solving the Navier-Stokes equations .....	752
 <b>PARTICLE METHODS .....</b>	 <b>759</b>
A numerical approach to model aggregate restructuring in shear flow using DEM in Lattice-Boltzmann simulations .....	761
Adaptive coarse-graining for large-scale DEM simulations.....	773
Novel efficient hybrid-DEM collision integration scheme.....	779
Implementing the kinetic theory of granular flows into the Lagrangian dense discrete phase model.....	785
Importance of the different fluid forces on particle dispersion in fluid phase resonance mixers .....	791
Large scale modelling of bubble formation and growth in a supersaturated liquid.....	798
 <b>FUNDAMENTAL FLUID DYNAMICS .....</b>	 <b>807</b>
Flow past a yawed cylinder of finite length using a fictitious domain method .....	809
A numerical evaluation of the effect of the electro-magnetic force on bubble flow in aluminium smelting process.....	819
A DNS study of droplet spreading and penetration on a porous medium.....	825
From linear to nonlinear: Transient growth in confined magnetohydrodynamic flows.....	831

# EXTREMELY FAST SIMULATIONS OF HEAT TRANSFER IN FLUIDIZED BEDS

Thomas LICHTENEGGER<sup>1,2\*</sup>, Stefan PIRKER<sup>1†</sup>

<sup>1</sup>Department of Particulate Flow Modelling, Johannes Kepler University, 4040 Linz, AUSTRIA

<sup>2</sup>Linz Institute of Technology (LIT), Johannes Kepler University, 4040 Linz, AUSTRIA

\* E-mail: thomas.lichtenegger@jku.at

† E-mail: stefan.pirker@jku.at

## ABSTRACT

Besides their huge technological importance, fluidized beds have attracted a large amount of research because they are perfect playgrounds to investigate highly dynamic particulate flows. Their overall behavior is determined by short-lasting particle collisions and the interaction between solid and gas phase. Modern simulation techniques that combine computational fluid dynamics (CFD) and discrete element methods (DEM) are capable of describing their evolution and provide detailed information on what is happening on the particle scale. However, these approaches are limited by small time steps and large numerical costs, which inhibits the investigation of slower long-term processes like heat transfer or chemical conversion.

In a recent study (Lichtenegger and Pirker, 2016), we have introduced recurrence CFD (rCFD) as a way to decouple fast from slow degrees of freedom in systems with recurring patterns: A conventional simulation is carried out to capture such coherent structures. Their re-appearance is characterized with recurrence plots that allow us to extrapolate their evolution far beyond the simulated time. On top of these predicted flow fields, any passive or weakly coupled process can then be investigated at fractions of the original computational costs.

Here, we present the application of rCFD to heat transfer in a lab-scale fluidized bed. Initially hot particles are fluidized with cool air and their temperature evolution is recorded. In comparison to conventional CFD-DEM, we observe speed-up factors of about two orders of magnitude at very good accuracy with regard to recent measurements.

**Keywords:** recurrent patterns, fluidized beds, multiphase heat and mass transfer, multiscale simulations .

## NOMENCLATURE

### Greek Symbols

$\alpha$  volume fraction,  $[\ ]$   
 $\Delta t$  time step,  $[s]$   
 $\rho$  density,  $[kg/m^3]$   
 $\boldsymbol{\tau}$  deviatoric stress tensor,  $[kg/s^2m]$

### Latin Symbols

$C$  specific heat capacity,  $[m^2/s^2K]$ .  
 $D$  diameter,  $[m]$ .  
 $D$  random fluctuations parameter,  $[m^2/s]$ .  
 $D$  dissimilarity norm,  $[\ ]$ .  
 $d\mathbf{w}$  random step,  $[m]$ .  
 $\mathbf{f}$  force density,  $[kg/s^2m^2]$ .  
 $\mathbf{F}$  force,  $[kgm/s^2]$ .

$k$  thermal conductivity,  $[kgm/s^3K]$ .  
 $m$  mass,  $[kg]$ .  
 $\dot{Q}$  heat transfer,  $[kg/s^3m]$ .  
 $R$  recurrence norm,  $[\ ]$ .  
 $t$  time,  $[s]$ .  
 $T$  temperature,  $[K]$ .  
 $\mathbf{u}$  field velocity,  $[m/s]$ .  
 $\mathbf{v}$  point velocity,  $[m/s]$ .

### Sub/superscripts

$f$  fluid.  
 $n$  normal.  
 $p$  particle.  
 $p$  pressure.  
 $rec$  recurrence.  
 $t$  tangential.  
 $v$  volume.

## INTRODUCTION

Modeling and simulation of fluidized beds is extremely demanding due to the various scales present. In the spatial domain, submillimeter particles are to be contrasted with the geometric dimensions of industrial-size plants. In the temporal domain, collisions set the lower limit of time scales at small fractions of a second while heat transfer or chemical conversion happens much more slowly.

Substantial progress has been made in up-scaling well-established mesoscopic methods like CFD-DEM (Cundall and Strack, 1979; Tsuji *et al.*, 1993) or the two-fluid model (TFM) (Anderson and Jackson, 1967; Gidaspow, 1994) to macroscopic sizes. To allow for coarser meshes so that larger systems can be described, sub-grid heterogeneities need to be modeled appropriately (Heynderickx *et al.*, 2004; Igci *et al.*, 2008; Igci and Sundaresan, 2011a,b; Milioli *et al.*, 2013; Ozel *et al.*, 2013; Parmentier *et al.*, 2012; Radl and Sundaresan, 2014; Schneiderbauer *et al.*, 2013; Schneiderbauer and Pirker, 2014; Wang *et al.*, 2008, 2010; Yang *et al.*, 2003; Zhang and VanderHeyden, 2002).

Although industrial-size reactors may be simulated with these methods, they are still bound to short-term investigations. Here, we show a systematic way to circumvent this problem and apply it to heat transfer in a lab-scale fluidized bed. In a recent paper, we introduced the idea of rCFD (Lichtenegger and Pirker, 2016) to time-extrapolate the behavior of systems dominated by reappearing structures. We use fields from short-term simulations with conventional

CFD-DEM or TFM to create long sequences of flow patterns with the aid of recurrence plots (Eckmann *et al.*, 1987).

On these sequences, we simulate heat transfer between gas and solid particles as measured by Patil *et al.* (Patil *et al.*, 2015) and obtain speed-up factors of about two orders of magnitude.

## MODEL DESCRIPTION

In the following, we briefly summarize the CFD-DEM method and refer the interested reader to extensive reviews (Deen *et al.*, 2007; Zhou *et al.*, 2010). Afterwards, the rCFD strategy is explained.

### Fluid equations

If a secondary, particulate phase is present, the Navier Stokes equations for a fluid with density  $\rho_f$  and velocity field  $\mathbf{u}_f$  become (Anderson and Jackson, 1967)

$$\frac{\partial}{\partial t} \alpha_f \rho_f + \nabla \cdot \alpha_f \rho_f \mathbf{u}_f = 0 \quad (1)$$

$$\frac{\partial}{\partial t} \alpha_f \rho_f \mathbf{u}_f + \nabla \cdot \alpha_f \rho_f \mathbf{u}_f \mathbf{u}_f = -\alpha_f \nabla p_f + \alpha_f \nabla \cdot \boldsymbol{\tau}_f + \mathbf{f}_{\text{drag}} + \mathbf{f}_{\text{ext}}. \quad (2)$$

Various correlations for particle-fluid drag  $\mathbf{f}_{\text{drag}}$  can be found in literature, we use one obtained from lattice-Boltzmann simulations (Beetstra *et al.*, 2007).

To picture heat transfer, we assume incompressible conditions and neglect contributions due to pressure variations to the enthalpy transport equation from which we derive

$$C_f^{(p)} \frac{\partial}{\partial t} \alpha_f \rho_f T_f + C_f^{(p)} \nabla \cdot \alpha_f \rho_f \mathbf{u}_f T_f = \nabla \cdot \alpha_f k_f^{(\text{eff})} \nabla T_f + \dot{Q}_{p-f}. \quad (3)$$

Both heat conduction  $\nabla \cdot \alpha_f k_f^{(\text{eff})} \nabla T_f$  and particle-fluid heat transfer  $\dot{Q}_{p-f}$  have to be modeled with empirical correlations (Syamlal and Gidaspow, 1985; Gunn, 1978). Note that for incompressible flows, Eq. (3) is decoupled from Eqs. (1) and (2) if density and viscosity are assumed to be temperature-independent.

### Particle equations

Solid particles are often modeled as perfect spheres which interact with each other via contact forces  $\mathbf{F}_i^{(p-p)}$ , with a surrounding fluid  $\mathbf{F}_i^{(p-f)}$  and possibly other sources  $\mathbf{F}_i^{(\text{ext})}$ . For each particle  $i$  with mass  $m_i$ , Newton's second law

$$m_i \dot{\mathbf{v}}_i = \mathbf{F}_i^{(p-p)} + \mathbf{F}_i^{(p-f)} + \mathbf{F}_i^{(\text{ext})} \quad (4)$$

determines its trajectory. The particle-particle force

$$\mathbf{F}_i^{(p-p)} = \sum_{j \neq i} (\mathbf{F}_{i,j}^{(n)} + \mathbf{F}_{i,j}^{(t)}) \quad (5)$$

on particle  $i$  due to all surrounding particles  $j$  consists of normal and tangential components which depend on the relative positions and velocities of  $i$  and  $j$  and are often described via spring-dashpot models (Cundall and Strack, 1979). The interaction of particles with a fluid  $\mathbf{F}_i^{(p-f)}$  is related to the drag force and the pressure gradient in Eq. (2).

Each particle is assumed to have a homogeneously distributed temperature  $T_i$ . We neglect particle-particle heat exchange because of the extremely short collision times so that only heat transfer from/to the fluid can change a particle's temperature via

$$m_i C_p^{(p)} \dot{T}_i = -\pi k_f D_i \text{Nu}_p (T_i - T_f(\mathbf{r}_i)) \quad (6)$$

in terms of the Nusselt number  $\text{Nu}_p$  (Gunn, 1978).

## Recurrence CFD

In a first step, we define norms for recurrence and dissimilarity of states, respectively, e.g.

$$R(t, t') \equiv 1 - \frac{1}{\mathcal{N}} \int d^3 r (\alpha_f(\mathbf{r}, t) - \alpha_f(\mathbf{r}, t'))^2 \quad (7)$$

$$D(t, t') \equiv 1 - R(t, t'), \quad (8)$$

to assess the similarity of flow fields obtained from the solution of Eqs. (1) – (4) at two times  $t, t' \leq t_{\text{max}}$ .

$$\mathcal{N} \equiv \max_{t, t'} \int d^3 r (\alpha_f(\mathbf{r}, t) - \alpha_f(\mathbf{r}, t'))^2 \quad (9)$$

ensures normalization in Eq. (7). We stress that it is an assumption that similarity according to Eq. (7) carries over to other fields like the particle velocity  $\mathbf{u}_p$ . As a matter of fact, it has to be checked *a posteriori* if they are sufficiently correlated to justify it.

Compared to binary recurrence statistics (Eckmann *et al.*, 1987), definition (7) allows for continuous degrees of similarity, which is referred to as unthresholded recurrence statistics (Marwan *et al.*, 2007).

Given a large enough recurrence statistics  $R(t, t')$ , it is possible to extrapolate the underlying system's behavior. Starting at some given begin time  $t_i^{(b)}$ , one randomly picks an interval of length  $\Delta t_i$ . In this study, we used uniformly distributed  $\Delta t_i$  in the range of  $t_{\text{max}}/20$  and  $t_{\text{max}}/5$ . Within  $\Delta t_i$ , the corresponding fields are taken as first elements of the desired sequence. Then, the most similar state to that at the end of the interval  $t_i^{(e)} = t_i^{(b)} + \Delta t_i$  is identified with the aid of  $R(t, t')$  and reconstruction is continued from there on. Again, an interval length is chosen and its fields are appended to the sequence. Obviously, this procedure can be repeated arbitrarily often. Figure 2 shows an example of two states that could be identified with each other because of a sufficiently high degree of similarity.

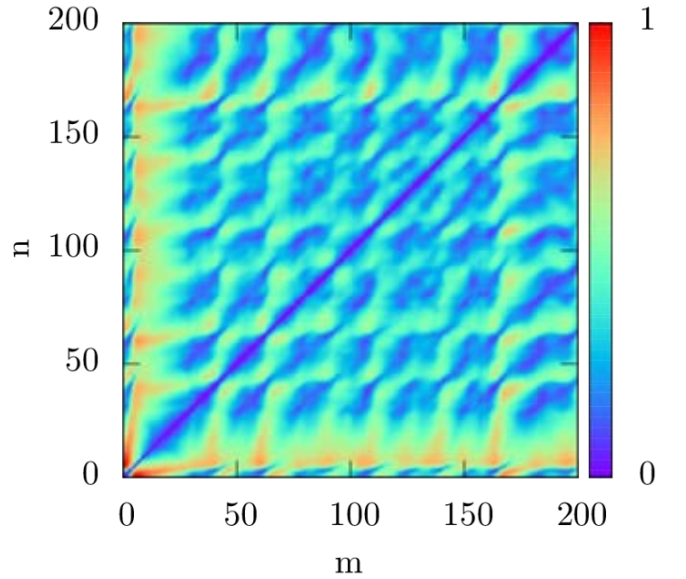


**Figure 1:** Degree of dissimilarity  $D(t, t')$  for the first 5 s of simulation of a fluidized bed corresponding to 200 snapshots. Besides the main diagonal with dissimilarity 0, a pattern of local minima and maxima is clearly visible, corresponding to more or less similar states. Their alignment approximately parallel to the main diagonal indicates pseudo-periodic behavior.

Finally, any passive processes can now be simulated on these fields in an extremely efficient way. The CFD-side problem of Eqs. (1), (2) and (3) is replaced with the temperature equation (3) alone. Other information like volume fraction, density and velocity are obtained from the recurrence process, only the temperature distribution is really calculated. The motion of the particles is simplified with tracers that follow the solid phase's velocity field  $\mathbf{u}_p^{(\text{rec})}$  and undergo random fluctuations  $d\mathbf{w}_i$ , viz.

$$d\mathbf{r}_i = \mathbf{u}_p^{(\text{rec})}(\mathbf{r}_i, t)dt + \sqrt{2D^{(\text{rec})}(\mathbf{r}_i, t)}d\mathbf{w}_i. \quad (10)$$

The latter act to avoid too high tracer concentrations in comparison to actual solid particles. A phenomenological, possibly position-dependent parameter  $D^{(\text{rec})}$  controls the strength of the fluctuations, e.g. via

$$D^{(\text{rec})}(\mathbf{r}, t) = D_0 \frac{\max[\alpha_p(\mathbf{r}, t) - \alpha_p^{(\text{rec})}(\mathbf{r}, t), 0]}{\alpha_p(\mathbf{r}, t)}. \quad (11)$$

The constant  $D_0$  has to be chosen empirically such that neither excessive clustering occurs nor that particle diffusion is enhanced dramatically. In neither case, the passive process under consideration could be pictured accurately.

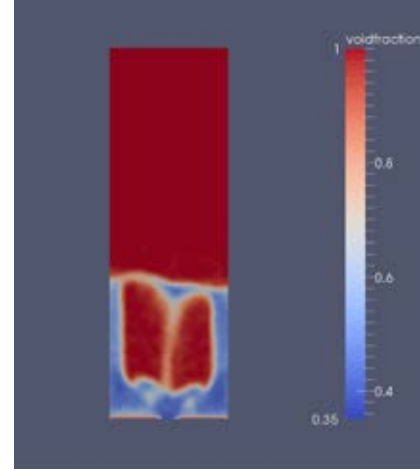
## SIMULATION SETUP

We set up simulations in close resemblance to recent experiments and simulations of heat transfer in a fluidized bed (Patil *et al.*, 2015) which we took as reference data. A  $8\text{ cm} \times 1.5\text{ cm} \times 25\text{ cm}$  cuboid was discretized into  $35 \times 110 \times 6$  equal cells and approximately 57000 1-mm spheres with material values of glass and initial temperature  $T_p^{(0)} = 90^\circ\text{C}$  were inserted. Air with ambient temperature  $T_f^{(0)} = 20^\circ\text{C}$  fluidized them with a superficial inlet velocity of  $u_{\text{inlet}} = 1.2\text{ m/s}$  and slowly cooled them.

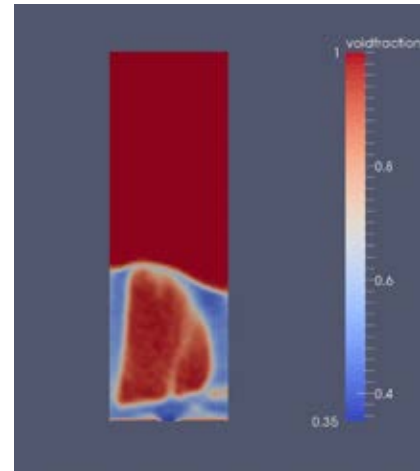
Since unresolved CFD-DEM requires larger cells than particles, the above grid could not be used to resolve the flux of heat through the domain walls happening over a very thin layer. Instead, its thickness was introduced as modeling parameter within reasonable bounds to control heat loss through the walls (Patil *et al.*, 2015). Since the focus of this work was rather the comparison of full CFD-DEM with rCFD than with experiments, we chose its value (in roughly the same range, but somewhat larger) such that our CFD-DEM results were in agreement with the reference simulation. We opted for this procedure because in contrast to the reference simulation which was carried out for an ideal, compressible gas, we approximated the system as incompressible to enable a recurrence-based treatment. Future work will address this shortcoming (Lichtenegger *et al.*, 2017) and allow for a meaningful comparison with measurements.

For the full CFD-DEM simulations, Eqs. (1) – (3) were solved under incompressible conditions employing the PISO algorithm (Issa, 1986). On the DEM side, we used velocity-Verlet integration (Verlet, 1967) for Eq. (4). The full CFD-DEM simulations were carried out for 10 s process time, the first 5 s were then used as basis for rCFD. We stress that this duration was chosen quite generously and smaller recurrence statistics would probably work equally well.

In this study, each particle was represented by exactly one tracer. Of course, one could also employ a parcel approach to combine clusters of particles into fewer tracers or conversely try to resolve coarse-grained CFD-DEM data with higher numbers of tracers.



(a)



(b)

**Figure 2:** Example of two equivalent states in the sense of dissimilarity norm Fig. 1. Although the volume fraction fields are not identical, they are close enough so that substituting one with the other does not lead to any significant inaccuracies.

Special care had to be taken with the choice of the fluctuation control parameter  $D_0$ . We found empirically that with  $d\mathbf{w}$  distributed uniformly on the unit sphere,  $D_0 = 10^{-4} \text{ m}^2/\text{s}$  was large enough to avoid too high particle concentrations and sufficiently small not to increase particle diffusion and consequently heat transfer and the mean cooling rate.

## RESULTS

According to the rCFD strategy outlined above, the first quantity to look at is the dissimilarity norm (or equally useful the recurrence norm) displayed in Fig. 1. 200 snapshots corresponding to 5 s real time are compared with each other, leading to a structure of local minima and maxima approximately parallel to the main diagonal. These minima are caused by very similar states that evolve in an analogous fashion, which demonstrates local pseudo-periodicity.

The degree of similarity is indicated in Fig. 2. Two volume fraction fields which give rise to a local minimum in the dissimilarity norm are shown. While small quantitative differences can be found, their qualitative features clearly agree: a large bubble was formed in the center of the bed with a few particles moving downwards in the middle of the bubble.

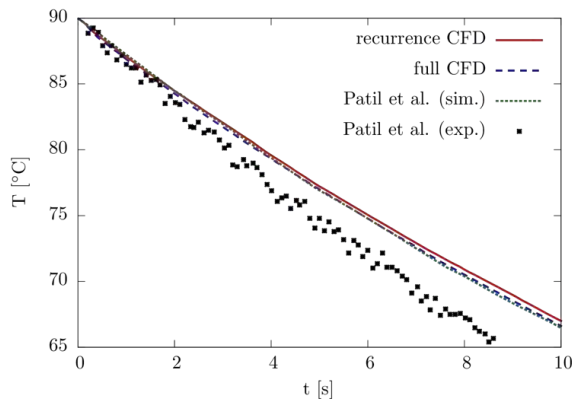


**Figure 3:** Particle mean temperature over time. Per construction, the full CFD simulations closely resembled the reference data (Patil *et al.*, 2015). As a consequence, the cooling rate was somewhat too low in comparison with measurements. Most importantly, recurrence CFD led to almost identical results as the full model.

If such semiquantitative agreement was sufficient to obtain a meaningful extrapolation of the fluidized bed's evolution is finally answered by looking at the particle mean temperatures from full and recurrence-based simulations in Fig. 3. As discussed above, the thickness of the boundary layer over which temperature drops to its wall value allowed for some "tuning" of the cooling rate. With a value to match the reference data (Patil *et al.*, 2015), the agreement of the present CFD-DEM results with them was of course to be expected. More importantly, however, the curves from rCFD and CFD-DEM agree very well. After 10 s their deviation is much less than  $1^\circ\text{C}$  at a speed-up of approximately two orders of magnitude.

Furthermore, Fig. 3 demonstrates that particle cooling happened over much longer times than the bed's fast dynamics. Such a clear separation of scales is clearly vital for the rCFD procedure because it minimizes the impact of switching between most similar but nevertheless different flow states on the passive process under consideration.

## CONCLUSION AND OUTLOOK

In this paper, we have demonstrated how to decouple the fast dynamics of a fluidized bed from the much slower heat transfer between solid particles and surrounding gas to accelerate the calculations. To facilitate the procedure, we assumed incompressible conditions in contrast to the treatment in the reference simulation (Patil *et al.*, 2015) and used a tuning parameter for wall heat loss to match our full CFD-DEM simulations to them. Upon these results, we built the recurrence statistics used for rCFD.

Future work (Lichtenegger *et al.*, 2017) will deal with rCFD for the compressible case, where we expect a superposed transient behavior due to a slow decrease of the mean gas temperature in the center of the bed. Besides more realistic results from the CFD-DEM calculation for a meaningful comparison with measurements, this will allow to study the bed over much longer times. Furthermore, a detailed performance analysis of the method's implementation might reveal optimization potential for even faster simulations.

## ACKNOWLEDGEMENT

This work was partly funded by the Linz Institute of Technology (LIT), Johannes Kepler University, Linz. We furthermore acknowledge support from K1-MET GmbH metallurgical competence center.

## REFERENCES

- ANDERSON, T.B. and JACKSON, R. (1967). "A fluid mechanical description of fluidized beds. Equations of motion". *Ind. Eng. Chem. Fundam.*, **6(4)**, 527–539.
- BEETSTRA, R., VAN DER HOEF, M.A. and KUIPERS, J.A.M. (2007). "Drag force of intermediate Reynolds number flow past mono- and bidisperse arrays of spheres". *AIChE J.*, **53(2)**, 489–501.
- CUNDALL, P.A. and STRACK, O.D.L. (1979). "A discrete numerical model for granular assemblies". *Géotechnique*, **29(1)**, 47–65.
- DEEN, N.G., VAN SINT ANNALAND, M., VAN DER HOEF, M.A. and KUIPERS, J.A.M. (2007). "Review of discrete particle modeling of fluidized beds". *Chem. Eng. Sci.*, **62(1-2)**, 28–44.
- ECKMANN, J.P., KAMPHORST, S.O. and RUELLE, D. (1987). "Recurrence plots of dynamical systems". *Europhys. Lett.*, **4(9)**, 973–977.
- GIDASPOW, D. (1994). *Multiphase flow and fluidization: continuum and kinetic theory descriptions*. Academic press.
- GUNN, D. (1978). "Transfer of heat or mass to particles in fixed and fluidised beds". *Int. J. Heat Mass Transfer*, **21(4)**, 467–476.
- HEYNDERICKX, G.J., DAS, A.K., DE WILDE, J. and MARIN, G.B. (2004). "Effect of clustering on gas-solid drag in dilute two-phase flow". *Ind. Eng. Chem. Res.*, **43(16)**, 4635–4646.
- IGCI, Y. and SUNDARESAN, S. (2011a). "Constitutive models for filtered two-fluid models of fluidized gas-particle flows". *Ind. Eng. Chem. Res.*, **50(23)**, 13190–13201.
- IGCI, Y. and SUNDARESAN, S. (2011b). "Verification of filtered two-fluid models for gas-particle flows in risers". *AIChE J.*, **57(10)**, 2691–2707.
- IGCI, Y., ANDREWS, A.T., SUNDARESAN, S., PANNALA, S. and O'BRIEN, T. (2008). "Filtered two-fluid models for fluidized gas-particle suspensions". *AIChE J.*, **54(6)**, 1431–1448.
- ISSA, R.I. (1986). "Solution of the implicitly discretised

- fluid flow equations by operator-splitting". *J. Comput. Phys.*, **62(1)**, 40–65.
- LICHTENEGGER, T., PETERS, E.A.J.F., KUIPERS, J.A.M. and PIRKER, S. (2017). "A recurrence CFD study of heat transfer in a fluidized bed". in preparation.
- LICHTENEGGER, T. and PIRKER, S. (2016). "Recurrence CFD - a novel approach to simulate multiphase flows with strongly separated time scales". *Chem. Eng. Sci.*, **153**, 394–410.
- MARWAN, N., ROMANO, M.C., THIEL, M. and KURTHS, J. (2007). "Recurrence plots for the analysis of complex systems". *Phys. Rep.*, **438(5-6)**, 237–329.
- MILIOLI, C.C., MILIOLI, F.E., HOLLOWAY, W., AGRAWAL, K. and SUNDARESAN, S. (2013). "Filtered two-fluid models of fluidized gas-particle flows: New constitutive relations". *AIChE J.*, **59(9)**, 3265–3275.
- OZEL, A., FEDE, P. and SIMONIN, O. (2013). "Development of filtered Euler–Euler two-phase model for circulating fluidised bed: high resolution simulation, formulation and a priori analyses". *Int. J. Multiph. Flow*, **55**, 43–63.
- PARMENTIER, J.F., SIMONIN, O. and DELSART, O. (2012). "A functional subgrid drift velocity model for filtered drag prediction in dense fluidized bed". *AIChE J.*, **58(4)**, 1084–1098.
- PATIL, A.V., PETERS, E.A.J.F. and KUIPERS, J.A.M. (2015). "Comparison of CFD-DEM heat transfer simulations with infrared/visual measurements". *Chem. Eng. J.*, **277**, 388–401.
- RADL, S. and SUNDARESAN, S. (2014). "A drag model for filtered Euler–Lagrange simulations of clustered gas–particle suspensions". *Chem. Eng. Sci.*, **117**, 416–425.
- SCHNEIDERBAUER, S. and PIRKER, S. (2014). "Filtered and heterogeneity-based subgrid modifications for gas–solid drag and solid stresses in bubbling fluidized beds". *AIChE J.*, **60(3)**, 839–854.
- SCHNEIDERBAUER, S., PUTTINGER, S. and PIRKER, S. (2013). "Comparative analysis of subgrid drag modifications for dense gas–particle flows in bubbling fluidized beds". *AIChE J.*, **59(11)**, 4077–4099.
- SYAMLAL, M. and GIDASPOW, D. (1985). "Hydrodynamics of fluidization: prediction of wall to bed heat transfer coefficients". *AIChE J.*, **31(1)**, 127–135.
- TSUJI, Y., KAWAGUCHI, T. and TANAKA, T. (1993). "Discrete particle simulation of a two-dimensional fluidized bed". *Powder Technol.*, **77**, 79.
- VERLET, L. (1967). "Computer" experiments" on classical fluids. I. Thermodynamical properties of Lennard-Jones molecules". *Phys. Rev.*, **159(1)**, 98.
- WANG, J., GE, W. and LI, J. (2008). "Eulerian simulation of heterogeneous gas–solid flows in CFB risers: EMMS-based sub-grid scale model with a revised cluster description". *Chem. Eng. Sci.*, **63(6)**, 1553–1571.
- WANG, J., VAN DER HOEF, M.A. and KUIPERS, J.A.M. (2010). "Coarse grid simulation of bed expansion characteristics of industrial-scale gas–solid bubbling fluidized beds". *Chem. Eng. Sci.*, **65(6)**, 2125–2131.
- YANG, N., WANG, W., GE, W. and LI, J. (2003). "CFD simulation of concurrent-up gas–solid flow in circulating fluidized beds with structure-dependent drag coefficient". *Chem. Eng. J.*, **96(1)**, 71–80.
- ZHANG, D.Z. and VANDERHEYDEN, W.B. (2002). "The effects of mesoscale structures on the macroscopic momentum equations for two-phase flows". *Int. J. Multiph. Flow*, **28(5)**, 805–822.
- ZHOU, Z.Y., KUANG, S.B., CHU, K.W. and YU, A.B. (2010). "Discrete particle simulation of particle-fluid flow: model formulations and their applicability". *J. Fluid Mech.*, **661**, 482–510.